A THREE-COMPONENT SONIC ANEMOMETER/THERMOMETER SYSTEM FOR GENERAL MICROMETEOROLOGICAL RESEARCH

P. A COPPIN

CSIRO Division of Environmental Mechanics, Canberra, A.C.T., Australia

and

K. J. TAYLOR

CSIRO Division of Applied Physics, Lindfield, N.S.W., Australia

(Received 6 June, 1983)

Abstract. A three-component sonic anemometer/thermometer system has been developed. It employs single switched transducer pairs and the inverse timed pulse method to yield an absolute calibration. Microprocessor control and use of newly developed transducers give a very small parts cost. The path length of the instrument can be varied from 10 to 15 cm; output is available in digital or analog form. Temperature sensing, via a 5 μm tungsten resistance element, is integrated into the digital system. Wind tunnel and field results have confirmed the success of the prototype and a set of operational instruments has been constructed.

1. Introduction

The sonic anemometer is generally regarded as one of the best instruments for the study of atmospheric turbulence. Its features include linear dynamic response, lack of moving parts, good directional characteristics and a frequency response limited only by the sound path length.

The first sonic anemometers were large and expensive (Kaimal and Businger, 1963). Recent commercial devices have provided significant advances (Hanafusa *et al.*, 1980), but cost still remains a barrier to their more widespread use. Attempts have been made to develop inexpensive single-component anemometers for eddy-correlation work (Campbell and Unsworth, 1979; Shuttleworth *et al.*, 1982), but their usefulness is limited to the measurement of vertical fluxes of scalar quantities over semi-infinite, flat, uniform surfaces. However, knowledge of the streamwise, as well as the vertical, wind component is essential in any serious study of the structure of atmospheric turbulence, expressed, for example, in the equation of conservation of turbulent kinetic energy (Bradley *et al.*, 1981) or for measurements over sloping surfaces, close to rough surfaces or where flow distortion due to nearby objects or the instrument itself is present.

The impetus for the development of the sonic anemometer described in this paper comes from current research programs to study the behaviour of atmospheric turbulence over complex terrain (e.g., Bradley, 1980). Such studies require the measurement of both streamwise and vertical gradients of turbulence quantities, thus necessitating simultaneous deployment of several instruments at a number of locations. Unit costs of the anemometer must therefore be substantially less than those of current commercial

Boundary-Layer Meteorology **27** (1983) 27–42. 0006–8314/83/0271–0027$02.40.

devices, but the instrument must retain extremely high standards of resolution and stability. The anemometer must be capable of measuring all three wind components plus temperature, and its path length should range down to 10 cm to provide sufficient frequency response for measurements close to the surface.

The instrument described herein meets these requirements through state-of-the-art application of digital control techniques and components, a microprocessor and a newly developed acoustic transducer.

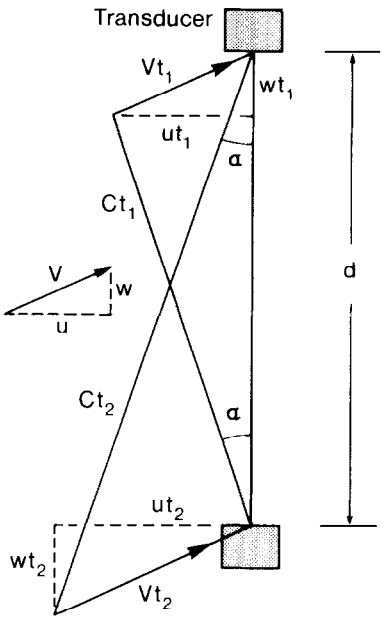

Fig. 1. Diagram of sound ray vectors showing principle of sonic anemometer operation.

2. Principle of Operation of Sonic Anemometers

Figure 1 illustrates the principle of operation of sonic anemometers. The time taken for a sound pressure wave to travel from the bottom to the top transducer in the presence of a wind vector V is given by

$$t_1 = \frac{d}{C\cos\alpha + w}\ ; \tag{1}$$

similarly in the other direction

$$t_2 = \frac{d}{C\cos\alpha - w}\ , \tag{2}$$

where d is the distance apart of the transducers, C the local speed of sound and w the component of the wind parallel to the transducer axis.

There are three basic ways of utilizing these relations to give an expression for w. Firstly, we can take the difference of the travel times

$$t_2 - t_1 = \frac{2dw}{C^2 - V^2} \approx \frac{2dw}{C^2} . \tag{3}$$

This gives a calibration which is a function of the distance apart of the transducers and the speed of sound squared. Since the speed of sound is a slowly varying function of atmospheric pressure, temperature and humidity, an instrument based on this method is liable to show drift in these parameters. In addition, the velocity components are contaminated by the rapid fluctuations in temperature and water vapour concentration, thus giving false cross-correlations (Freihe, 1976).

The travel times can be obtained from phase shift measurements, either using two pairs of transducers transmitting continuously in opposite directions (Kaimal and Businger, 1963) or using a single pair and switching the transducer functions (Shuttleworth *et al.*, 1982). The latter method has the advantage of removing any differences in path length in the two transducer pairs or phase lag in the associated circuitry. The travel times can also be obtained by direct measurement of the travel time of a sound pulse (Mitsuta, 1966; Kaimal *et al.*, 1974).

The second method is to take the difference of the inverse of the travel times

$$\frac{1}{t_2} - \frac{1}{t_1} = \frac{2w}{d} . \tag{4}$$

This gives a calibration which is a function only of the distance apart of the transducers, a so-called 'absolute' calibration. The only commercial sonic anemometers to use this principle are the newer KAIJO-DENKI DA series, which employ single transducer pairs and the timed pulse technique for obtaining the travel times (Hanafusa *et al.*, 1982). This method has probably not been more widespread due to the difficulty of obtaining the reciprocals of the travel times in real time.

The third method uses a slightly different technique. A phase lock loop (PLL) circuit is used to produce a signal whose frequency is changed to keep the received signal in phase with the transmitted one. Details of the method are clearly explained by Larson *et al.* (1979). In summary, assuming perfect phase lock, the following expression for w can be obtained

$$\left(\frac{\omega_2 - \omega_0}{\omega_0}\right) - \left(\frac{\omega_1 - \omega_0}{\omega_0}\right) = \frac{2w}{C_0} , \tag{5}$$

where ω_2 and ω_1 are the frequencies necessary to obtain perfect phase lock for the two travel directions, ω_0 is the free running frequency of the PLL in the absence of wind and C_0 the speed of sound at ω_0. The PLL circuit produces a signal which is linearly

proportional to $(\omega - \omega_0)/\omega_0$ so very simple circuitry can be used. The calibration is still dependent on C_0 but it is independent of d and immune from contamination due to fluctuations in temperature and humidity.

Two anemometers have employed this method, Larsen *et al.* (1979) using a dual transducer pair and Campbell and Unsworth (1979) a single transducer pair and a switching system. Problems with this method include considerable temperature drift in the PLL oscillator and demands placed on the phase behaviour of the transducers. The tracking of the PLL causes continually varying frequencies to be presented to the transducers; under these circumstances, resonant transducers will produce spurious phase shifts. With such drift problems, these anemometers, although low cost, are restricted to eddy-correlation measurements where the mean wind component is removed over a relatively short period of 15 to 30 min.

3. Instrument Design

Of the various methods for obtaining the wind vector outlined in the previous section, we decided to use pulse transmission, taking the inverse of the travel times (Equation (4)) and using a single, switched pair of transducers for each of the three wind axes. This method provides an absolute calibration of the instrument, and the use of a single transducer set for each axis ensures a similar path length d for each direction of sound transmission.

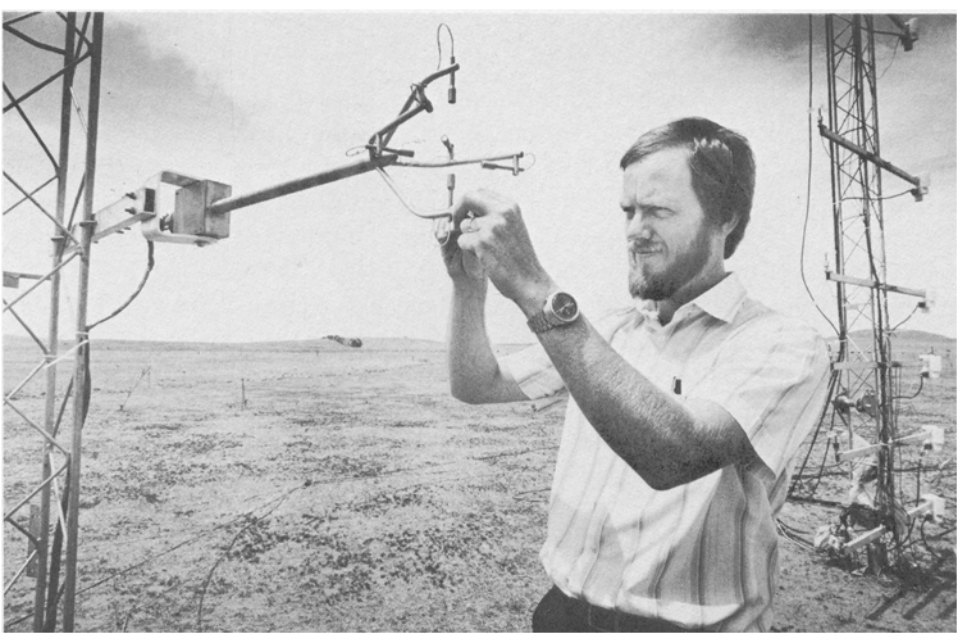

Fig. 2. Experimental arrangement for a field test of the sonic anemometer/thermometer system.

3.1. THE ARRAY

Any *in situ* measurement of a vector quantity such as wind velocity is subject to distortion by the presence of the instrument itself. Flow distortion leads to errors in measured correlations between wind components and between wind vector and scalar variables (Wyngaard, 1981; Wucknitz, 1980). One of the worst effects is the production of a mean tilt in the flow, where the fluctuations in horizontal velocity contaminate those in the vertical velocity; correction for this distortion is not a simple rotation of the coordinates (Wyngaard, 1981).

The array, shown in Figure 2, consists of the transducers and temperature sensor mounted at the end of a horizontal tube 50 cm long by 2.5 cm diameter. At the other end of the tube is a 12 × 10 × 5 cm box containing the preamplifier and pulse transmission circuits. The whole array is symmetric to prevent the generation of tilted flow, and the transducer arrangement and the extended mounting tube are designed to minimize blockage of flow.

The horizontal axes are mounted at the conventional 120° to allow a broad acceptance angle (e.g., Hanafusa *et al.*, 1980; Kaimal *et al.*, 1974). These axes are offset in the vertical by 4 cm and the intersection of their projection is offset towards the rearmost transducers; both these measures reduce mutual interference. The vertical axis is offset 3.5 cm in front of the intersection of the projected horizontal axes. Figure 3 shows this arrangement.

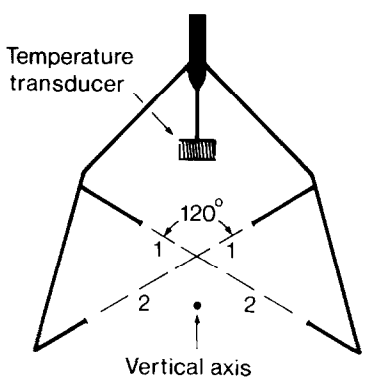

Fig. 3. Projection of sonic array axes.

The precision of the internal angles within the array is 0.1°. This reduces the possibility of contamination of the correlations between the various wind components to a satisfactory level (Kaimal *et al.*, 1974).

The path length is a compromise between frequency response and directional response to a changing wind vector. The transducers produce wake interference when the wind is at a large angle to the measurement axis, thus reducing the measured wind velocity. The farther apart the transducers, the less this interference contributes to the velocity. The prototype had a fixed path length of 10 cm, but the working model has a path length

that is adjustable between 10 and 15 cm. The transducers are mounted on extendable stalks of 5 mm diameter, the extension being 6.5 cm for a path length of 10 cm.

3.2. THE TRANSDUCERS

The sonic anemometer described in this paper uses a new transducer developed for the instrument at the CSIRO Division of Applied Physics. The transducer, for which a patent is pending, is an electrostatic device with a body diameter of 11 mm and a length of approximately 10 mm. The diaphragm, 10 mm in diameter, is made from 6 μm polyester film with a thin, vacuum-coated gold film. A protective, acoustically transparent mesh is placed across the transducer face. The pole piece is a specially designed backing plate which tailors the frequency response to the required range and flatness. The bias voltage is 200 V and the driving voltage applied is $\pm$ 14 V. The frequency response is substantially flat from 50 kHz to 150 kHz. The transducer features excellent damping with a received 100 kHz sound pulse effectively extinguished within a few cycles.

The low driving voltages allow the use of CMOS analog switches and solid-state relays to create the drive signal and handle switching functions. These switches can be easily controlled by conventional digital logic, permitting the implementation of low cost microprocessor control techniques in the design. The transducer construction is simple enough to permit manufacture of large numbers.

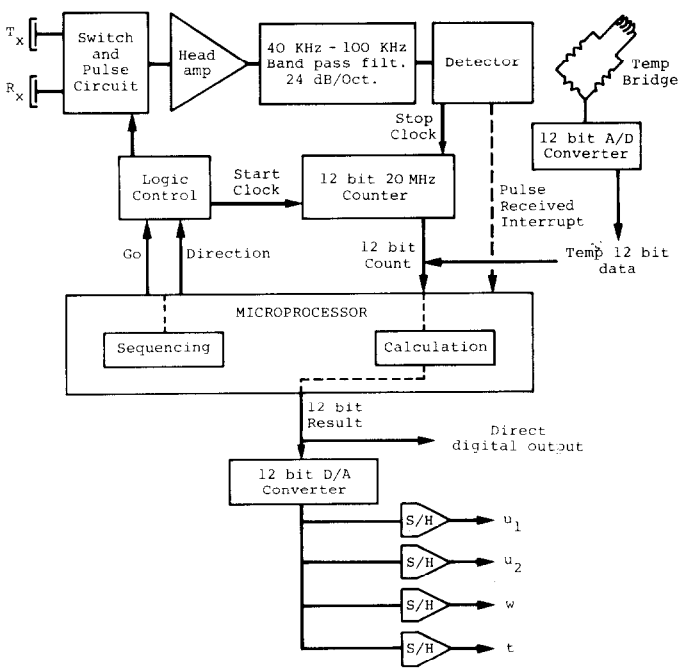

Fig. 4. Sonic anemometer/thermometer system block diagram.

3.3. Operation of the Anemometer

The anemometer function, based on Equation (4), involves the timing of a sound pulse as it travels, first in one direction and then the other, between the two transducers that form each wind measuring axis. The three axes are operated in turn.

The instrument is controlled by a low cost, single board microcomputer (SYNERTEK SYM 1). The operating sequence is shown in the system block diagram (Figure 4) and the timing diagram (Figure 5). The microcomputer sets the direction of sound travel via the switching circuits and then sends a 'go' signal to the logic circuits, an operation that generates the sound pulse and resets and starts a 12 bit binary computer that is fed by a 20 MHz oscillator.

The received signal is processed via an impedance matching circuit, a preamplifier and a 25 dB/Oct, 60–100 kHz band pass filter. The signal at the input to the detector is seen as a rapidly rising wave packet, which is damped within a few cycles (shown in schematic form in Figure 5).

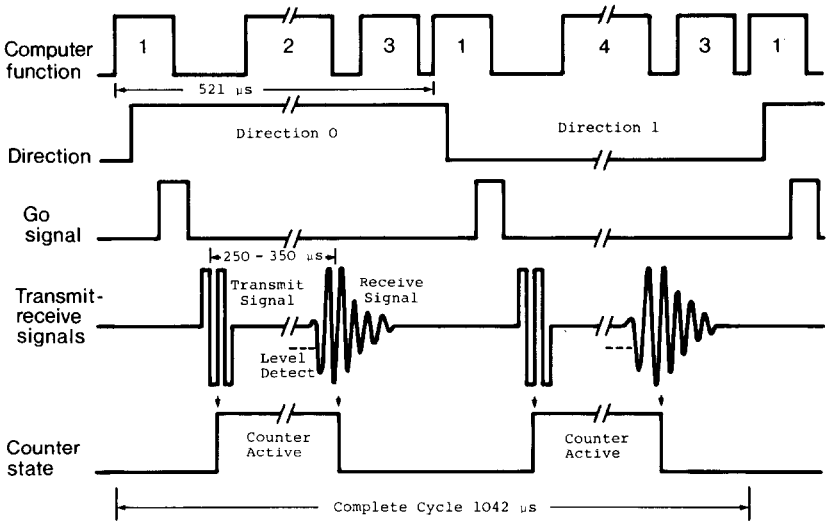

Fig. 5. Sonic anemometer system timing diagram. A cycle for one axis, which results in a wind speed measurement, is shown. Computer function coding: (1) set direction, send go; (2) calculate previous wind axis, average, and output if complete; (3) fetch count and store; (4) fetch temperature, average, and output if complete.

The detection circuit is disabled until the earliest possible arrival time of the sound pulse. The first major negative-going wave front is used to trigger a comparator which, in turn, activates a zero-crossing detector. The second positive-going zero crossing after the level detect (on the largest wave and hence the least sensitive to noise) is used to stop the counter. This scheme was adopted in preference to a simple level detect, as the position of a given level on a wave front is a function of wave amplitude, whereas the position of the zero crossing is invariant.

The detection of the sound pulse also sends an interrupt to the microcomputer, which reads the counter and stores the value. The direction of sound travel is reversed and the procedure repeated. When both directions have been completed, the whole sequence is repeated for the next wind axis. During the transit time of this next sound pulse, the microcomputer calculates the wind component from the travel time measurements for the previous axis.

The travel times read from the counter are inverted via a lookup table stored in memory. Scaling for the maximum windspeed is performed via the lookup table, so maximum windspeeds of 10 or 20 m s^{-1} can be selected by loading the appropriate lookup table. The travel times for a maximum wind velocity of 20 m s^{-1} vary between 250 and 350 μs. For a 20 MHz clock, this means that the count will lie between 5000 and 7000 so that a lookup table of only 2000 values need be stored. Note that as the 12 bit counter has a range of 4096, the counter is allowed to overflow once.

The difference of the reciprocal travel times is taken and the answer accumulated for each wind axis. The microcomputer averages 16 readings to improve resolution and produces the result, either as a 12 bit number with channel identification via a digital interface or as an analog signal via a 12 bit D/A converter, the latter primarily for monitoring purposes.

The analog output for the three wind signals and the temperature signal are generated with the same D/A converter and are held on separate sample and hold circuits.

The interval between pulse firings is 521 μs; a wind reading is therefore available for all the axes after 3.126 ms. The average of sixteen wind readings per result yields a net rate of 20 Hz per channel at the digital output. The analog signal is passed through a low pass filter with a half-power point of 10 Hz.

The cycling of the three axes of wind measurement allows circuitry to be shared. The three pairs of transducers retain their own preamplifier and pulse firing circuitry, so that their impedances can be matched, but share logic control, filter, detector and counter circuits. Extra switches select the preamplifier and firing circuit connected to the common filter/detector and logic circuits, respectively.

The separate preamplifier circuits are mounted in the small box on the sonic array body itself (see Section 3.1 and Figure 2). The signals travel approximately 70 cm to and from the transducers. A 5 m cable connects the instrument body to an intermediate box of electronics (27 × 18 × 13 cm) that houses the filter/detector, logic control, counter and temperature transducer electronics. The cable that connects this intermediate box to a third box containing the microcomputer carries only the 12 bit data bus and digital control lines. Being a digital only line, it is inherently noise free and its length is limited only by the capabilities of the line drivers used. The prototype has been successfully run using 400 m of cable, although the theoretical maximum is well in excess of this. All critical timing is done in the intermediate electronics box.

For a path length of 10 cm, the 20 MHz clock rate gives a basic resolution of ± 2.5 cm s^{-1} for each individual wind reading. Averaging gives an improvement by a factor of $\sqrt{n}$, where n is the number of readings averaged, i.e., a factor of 4 when 16 readings are averaged. Thus, a resolution of approximately ± 0.6 cm s^{-1} at the 20 Hz

digital output is achieved. Faster analog and digital outputs are available by changing the degree of averaging of the signals within the microcomputer. The analog filtering can be adjusted accordingly.

3.4. The temperature sensor

The temperature sensor consists of a 5 μm tungsten wire, approximately 50 cm long, wound on an open cylindrical form 4 cm by 2 cm diameter (Wesely *et al.*, 1970), which is mounted on a 6 cm stalk of diameter 0.42 cm. The stalk is mounted within the array and projects from the end of the mounting tube (see Figures 2 and 3). The wire resistance is about 1500 ohm, and a voltage output is obtained using a simple Wheatstone bridge with a ratio of 20 : 1 and a power supply of 10 V. Self-heating of the wire due to the current is below 0.01 °C at zero wind speed; solar radiation loading of the fine wire is negligible.

An instrumentation amplifier buffers the bridge and provides selectable gain so that the full scale range of a 12 bit A/D converter that follows the amplifier is either 10 or 20 °C. The bridge and A/D converter are mounted on a single circuit board, which is housed in the intermediate electronics box. The A/D converter is activated by the 'go' pulses fed to the sonic anemometer logic and its output shares the same 12 bit data bus as the anemometer section via a tristate buffer system. The resultant data are read by the microcomputer during the 'off' cycle in the wind measurement. The wind vector from a given axis is calculated during the transit time of the sound pulse for the first transmit direction of the next axis. The transit time during the second direction is hence free for reading and output of temperature data (see timing diagram, Figure 3).

Temperature data are also averaged over sixteen readings and output at 20 Hz. Overall resolution of the temperature system is better than 0.01 °C.

An interesting possibility generated by the free time available in the cycle is the ability to add further transducers. The cycling through three wind components creates three periods of free time, only one of which is used by the temperature sensor. Two other signals, possibly humidity or pressure signals, can be added to the digital system. One group of scientists using a version of the anemometer has incorporated an infrared absorption hygrometer signal into the system by using a multi-channel A/D converter system in place of the single channel one used for the temperature bridge (Trevitt, 1983, personal communication).

3.5. Construction costs and future developments

The parts cost of the main anemometer/thermometer system, excluding the transducers, is approximately $A1000 for a digital output system and $A1300 with additional analog outputs. Of this amount, $A250 is for the SYM1 microcomputer. This is based on low volume parts costs at the time of writing. To this must be added the cost of the 20-conductor shielded main digital bus cable, which is $A290 per 100 m.

Negotiations are underway for commercial manufacture of the instrument in various configurations.

Development is proceeding of a digital-only version of the anemometer/thermometer with the SYM1 microcomputer replaced by a single chip version housed in the intermediate electronics box. Communication to a data logger is via an inexpensive RS232 serial link. This eliminates the present microcomputer box, the expensive digital bus cable and reduces the associated construction time.

4. Instrument Performance

4.1. Laboratory tests

A range of laboratory tests was performed on the three-dimensional prototype, including measurements of offsets, drift, temperature dependence and noise levels. A PDP11/23 minicomputer was used to accept the digital output data from the anemometer and perform the necessary on-line statistical calculations. All tests were performed with the array in a small windproof enclosure.

Initial tests showed that the received sound pulse had a signal-to-noise ratio in excess of 40 dB, which placed the noise-induced uncertainty of the zero crossing point below the resolution of the 20 MHz counter. Hence, the noise level at the digital output is that predicted on theoretical grounds from the counter uncertainty, i.e., $\pm$ 0.6 cm s^{-1}.

As shown in Equation (4), the path length d is the major variable in the calibration. Thermal expansion of the array could affect this value; a 40 °C range in array temperature, however, would change the calibration slope by only 0.06%.

Sound pulses sent and received in both travel directions share the same electronics throughout; however, an offset in the calibration arose because the pair of transducers had different phase delays for each direction. This offset, equivalent to a few cm s^{-1}, was invariant with time over several months of testing. The temperature sensitivity of this phase-related offset was tested in a controlled temperature room over a 0 °C to 40 °C range and was negligible.

Errors can also arise when an electronic delay or change in delay is added to the travel times for both directions, i.e.,

$$\frac{1}{t_2 + \Delta t} - \frac{1}{t_1 + \Delta t} = \frac{t_1 - t_2}{t_2 t_1 \left(1 + \left(\frac{t_1 + t_2}{t_1 t_2}\right)\Delta t + \Delta t^2\right)}$$

$$\approx \frac{2w}{d\left(1 + \left(\frac{t_1 + t_2}{t_1 t_2}\right)\Delta t\right)} . \tag{6}$$

The delay through the electronic circuitry between the transducers and the detector was approximately 12 μs compared to a typical travel time of 300 μs. A delay of this permanent nature would cause a desensitizing of the calibration of about 8.0%. The measured delay, invariant with time and temperature, is therefore subtracted from travel times for both directions by the microcomputer before the inverse is obtained. If, for

some reason, the delay drifts by 1 μs, a substantial change, the calibration will drift by only 0.6%.

4.2. WIND TUNNEL TESTS

Wind tunnel tests were performed in the Division's 1.8 × 0.8 m wind tunnel (Wooding, 1968) with a pitot tube and precision differential pressure transducer as the reference for wind speed. Horizontal axes were calibrated by facing the instrument directly into the wind, so that the airflow was inclined 60° to each sonic axis.

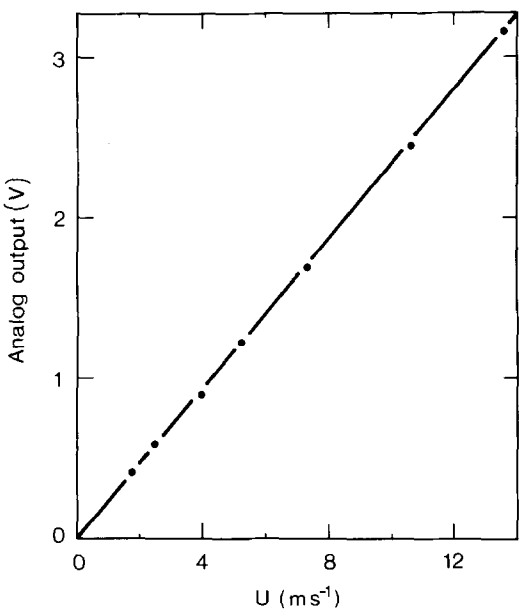

Fig. 6. Calibration of single sonic anemometer axis placed at 30° to flow.

Figure 6 shows a typical calibration. The slope is linear to within the accuracy of the reference system (1%); calibrations over several months showed slopes within 1% of each other. The intercept at zero wind reflects the small offsets previously mentioned. The slope of the calibration is 3% less than the theoretical value based on the path length. This is probably due to the end effects produced by the transducers, as outlined in Section 3.4. A similar effect was observed by Hanafusa *et al.* (1982) for their anemometer, which uses the same principle of operation.

The angular variation in the response of a single sonic axis is shown in Figure 7 as a fraction of a perfect cosine function. Here the azimuth is defined as the angle relative to the normal to the sonic axis. The reading at 20° azimuth was taken to be correct. The behaviour is close to ideal between ± 20° and within 10% to ± 50°. The vertical angle of attack of flux-carrying eddies rarely exceeds ± 30°, except under very unstable conditions or close to rough surfaces where high turbulent intensities are encountered (McBean, 1974).

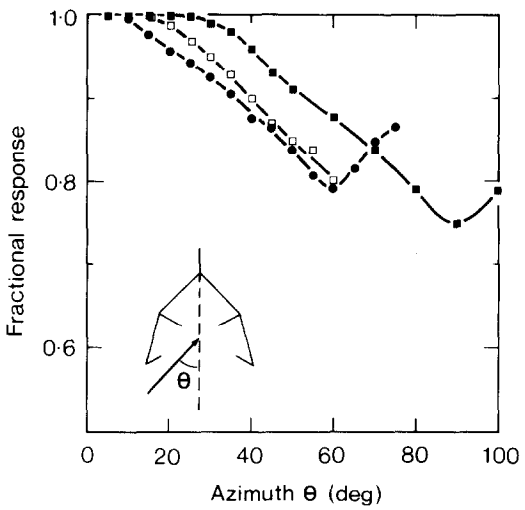

Fig. 7. Sonic anemometer cosine response fraction as a function of azimuth. (■) Single axis response as a function of azimuth relative to normal to single sonic axis. (●) Horizontal vector response calculated from two horizontal axes (Equation (9)) as a function of true azimuth. (□) Horizontal vector response for sonic anemometer with 10 cm path length (Hanafusa *et al.*, 1982).

A more severe effect of this cosine response is on the total horizontal wind vector calculated from the two horizontal axes. The downwind and crosswind components, u and v, of the total vector are computed from the horizontal axes by virtue of their 120° included angle, as follows:

$$u = V_1 + V_2 , \tag{7}$$

$$v = (V_1 - V_2)/\sqrt{3} , \tag{8}$$

where V_1 and V_2 are the two horizontal axial flows.

The total horizontal wind vector is specified by its magnitude U_T and azimuth ϕ, which are given by

$$U_T = \sqrt{(u^2 + v^2)} , \tag{9}$$

$$\phi = tan^{-1}\left(\frac{v}{u}\right)$$

$$= tan^{-1}\left(\frac{V_1 - V_2}{\sqrt{3}\,(V_1 + V_2)}\right) . \tag{10}$$

Figure 7 shows the total measured wind vector, expressed as a fraction of true cosine response, plotted as a function of true azimuth. Also shown are similar results for a KAIJO-DENKI DA series sonic anemometer with a path length of 10 cm (Hanafusa *et al.*, 1982).

The cosine response starts dropping immediately either side of zero azimuth. In the straight-ahead position, the normal to each axis is at 30° to the wind flow. The results for the single axis show the response to be good at this angle. As the azimuth increases, the angle of wind flow decreases to one axis and increases to the other. The worsening response of the axis experiencing the increasing angle results in a lower total vector reading. At an azimuth of ± 30°, the prototype anemometer (path length 10 cm) has a deficit of 7% compared to 5% for the 10 cm model of Hanafusa. This larger deficit is perhaps due to the long connector housing,which adds approximately 1.0 cm to the length of the transducer in the prototype shown in Figure 2. Subsequent models, however, feature a much shorter transducer body than the prototype and a thinner mounting stalk, both of which should improve cosine response. These models also have the facility for adjustment of the path length over the range 10 to 15 cm.

Deficiencies in horizontal directional response appear to be a major limitation in the field use of sonic anemometers. However, Hanafusa *et al.* (1982) show that these deficiencies have negligible effect on the measured turbulence statistics. They suggest that the discrepancy is due to the use of laminar flow in the wind tunnel tests. Laminar flow allows transducer wakes to persist, yielding poor directional response, whereas the atmospheric turbulence present during field use causes the wakes to decay much faster.

4.3. Field tests

In the absence of an instrument of comparable or superior performance, field testing of the prototype anemometer/thermometer was restricted to broad comparisons with a set of profile instruments and verification and debugging of system functions under field conditions. However, some interesting phenomena were observed.

The prototype three-dimensional instrument was operated for several days at the Division's field site at Bungendore, New South Wales. The site is substantially flat with a very low roughness due to prolonged drought conditions. The instrument was mounted on a 6 m mast of 20 cm triangular section at a height of 2 m. The mounting was such that the anemometer measuring volume was 90 cm from the nearest edge of the mast (Figure 2). A similar 26 m mast containing profile anemometers and psychrometers was located a few metres to one side of the sonic's mast. Conditions during testing were mainly hot (30 °C) and windy with a mean speed of 10 m s^{-1} or greater at the 2 m level.

The digital data transmission system operated with little degradation through 200 m of cable, having previously been tested successfully with 400 m in the laboratory. Measured shear stress results were sufficiently close to those derived (theoretically much less accurately) from the profile anemometers, indicating no gross performance problems. Values for u_* were generally within ± 10%, a good result for the unstable conditions encountered.

Figure 8 shows typical spectra of the velocity components obtained in unstable conditions. The position of the peak in the w spectrum and general shape of the spectra agree well with accepted forms for measurements over flat, uniform surfaces in unstable conditions (e.g., Kaimal *et al.*, 1972), with the $-5/3$ law rolloff evident up to the 5 Hz

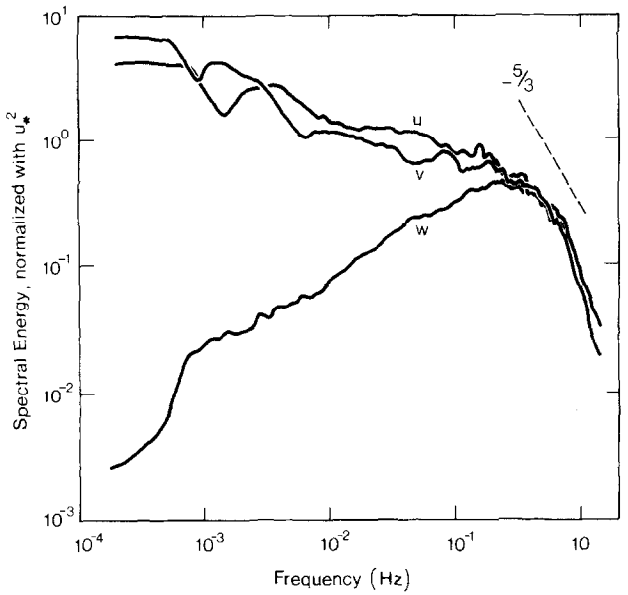

Fig. 8. Typical spectra of the three wind components u, v, w from sonic anemometer field tests.

turnover point of the filter in use at the time. Hence, there is no evidence of false peaks or other effects due to undetected interactions within the anemometer system.

An interesting phenomenon relates to flow distortion, as indicated by a measured tilt angle in the mean flow of 0.8°. It is difficult to explain the source of this tilt. The instrument itself is substantially symmetric in the vertical, as was the mounting hardware; however, the tower itself was not, being an object of fixed length mounted on a plane surface. The tilt angle increased to approximately 1.5° when a Lyman-alpha response hygrometer was placed some 10 cm below and 10 cm behind the centre of the sonic measuring volume. This instrument could be regarded as a 20 cm long by 2.5 cm diameter cylinder placed across the flow.

The effect of this extra tilt in the mean flow was quite noticeable in the measured shear stress. The sonic-derived values for u_* before the Lyman-alpha was mounted were consistently higher than the profile-derived values by an average of 5%. After the mounting of the hygrometer, the situation was reversed, the sonic values being consistently lower by some 7%. This decrease is consistent with the theory of Wyngaard (1981) for shear stress distortion ahead of and above a cylinder. This evidence reinforces the need for careful attention to the problem of probe-induced distortion.

5. Conclusion

A low-cost three-component sonic anemometer/thermometer system has been developed. Its specifications are summarized in Table I. The prototype anemometer has been

tested successfully in the wind tunnel and in the field; the calibration was invariant with time and second-order drifts were negligible. The single-axis cosine response was satisfactory, but the horizontal wind vector directional response was compromised to a small degree in the 10 cm path length model, although this may not be of consequence in field use. Field tests were limited but verified the general system performance and operation with long cables. A set of operational field instruments has been constructed on the basis of the success of the prototype.

TABLE I

Specifications of three-component sonic anemometer/thermometer system

Sonic Section	
Principle of operation:	Inverse timed pulse, absolute calibration
Acoustic path:	10 cm single switched transducer pair (15 cm available)
Range:	$\pm$ 20 m s^{-1}, higher or lower selectable
Digital output:	12 bit parallel binary plus 4 bit channel number
Analog output:	$\pm$ 5 V or $\pm$ 10 V full scale
Frequency response:	20 Hz digital output, 10 Hz analog output (variable)
Resolution:	$\pm$ 0.6 cm s^{-1} at 20 Hz
Calibration accuracy:	1% (determined by reference)
Array:	3-component – horizontal axes at 120 deg offset in vertical – vertical axis orthogonal
Temperature Section	
Principle of operation:	5 μm tungsten resistance wire in Wheatstone bridge
Wire resistance:	approx. 1500 ohm
Temperature range:	10 °C or 20 °C, selectable
Resolution:	Better than 0.01 °C
Output and frequency response:	same as sonic section

Acknowledgements

The authors would like to thank Garry Miller for his invaluable contribution to the electronics of the anemometer/thermometer system, Colin Hazelton for his patient work with the array construction, and the many other colleagues who contributed to the development of the instrument.

References

Bradley, E. F.: 1980, 'An Experimental Study of the Profiles of Wind Speed, Shearing Stress and Turbulence at the Crest of a large Hill', *Quart. J. Roy. Meteorol. Soc.* **106**, 101–123.

Bradley, E. F., Antonia, R. A., and Chambers, A. J.: 1981, 'Turbulence Reynolds Number and the Turbulence Kinetic Energy Balance in the Atmospheric Surface Layer', *Boundary-Layer Meteorol.* **21**, 183–197.

Campbell, G. S. and Unsworth, M. H.: 1979, 'An Inexpensive Sonic Anemometer for Eddy Correlation', *J. Appl. Meteorol.* **18**, 1072–1077.

Freihe, C. A.: 1976, 'Effects of Sound Speed Fluctuations on Sonic Anemometer Measurements', *J. Appl. Meteorol.* **15**, 607–610.

Hanafusa, T., Korobi, Y., and Mitsuta, Y.: 1980, 'Single Head Sonic Anemometer-Thermometer', WMO Instruments and Observing Methods, Report No. 3, Lower Tropospheric Data Compatibility, Geneva.

Hanafusa, T., Fujitani, T., Korobi, Y., and Mitsuta, Y.: 1982, 'A New Type Sonic Anemometer-Thermometer for Field Operation', *Papers in Meteorol. and Geophys.* **33**, 1–19.

Kaimal, J. C. and Businger, J. A.: 1963, 'A Continuous Wave Sonic Anemometer-Thermometer', *J. Appl. Meteorol.* **2**, 156–164.

Kaimal, J. C., Wyngaard, J. C., Izumi, Y., and Cote, O. R.: 1972, 'Spectral Characteristics of Surface Layer Turbulence', *Quart. J. Roy. Meteorol. Soc.* **98**, 563–589.

Kaimal, J. C., Newman, J. T., Bisberg, A., and Cole, K.: 1974, 'An Improved Three Component Sonic Anemometer for Investigation of Atmospheric Turbulence', in R. B. Dowdell (ed.), *Flow: Its Measurement and Control in Science and Industry*. Vol. 1, Instrument Society of America, Pittsburgh, PA, pp. 349–359.

Larson, S. E., Weller, F. W., and Businger, J. A.: 1979. 'A Phase Locked Loop Continuous Wave Sonic Anemometer Thermometer', *J. Appl. Meteorol.* **18**, 562–568.

McBean, G. A.: 1974, 'The Turbulent Transfer Mechanisms: A Time Domain Analysis', *Quart. J. Roy. Meteorol. Soc.* **100**, 53–56.

Mitsuta, Y.: 1966, 'Sonic Anemometer for General Use', *J. Meteorol. Soc. Jap.* **44**, 12–24.

Shuttleworth, W. J., McNeill, D. D., and Moore, C. J.: 1982, 'A Switched Continuous Wave Sonic Anemometer for Measuring Surface Heat Fluxes', *Boundary-Layer Meteorol.* **23**, 425–448.

Trevitt, C.: 1983, Personal Communication, CSIRO Div. of Plant Industry, Canberra, Australia.

Wesely, M. L., Thurtell, G. W., and Tanner, C. B.: 1970, 'Eddy Correlation Measurements of Sensible Heat Flux near the Earth's Surface', *J. Appl. Meteorol.* **9**, 45–50.

Wooding, R. A.: 1968, 'A low Speed Wind Tunnel for Model Studies in Micrometeorology', Australia CSIRO Div. Plant Industry Tech. Pap. No. 25, pp. 1–39.

Wucknitz, J.: 1980, 'Flow Distortion by Supporting Structures', in F. Dobson and L. Hasse (eds.), *Air Sea Interaction, Instruments and Methods*, Plenum Press, New York, pp. 605–626.

Wyngaard, J. C.: 1981, 'The Effects of Probe-Induced Distortion in Atmospheric Turbulence Measurements', *J. Appl. Meteorol.* **20**, 784–789.